Figure S1

a **PACT clearing progression in 2 mm rat brain slices**

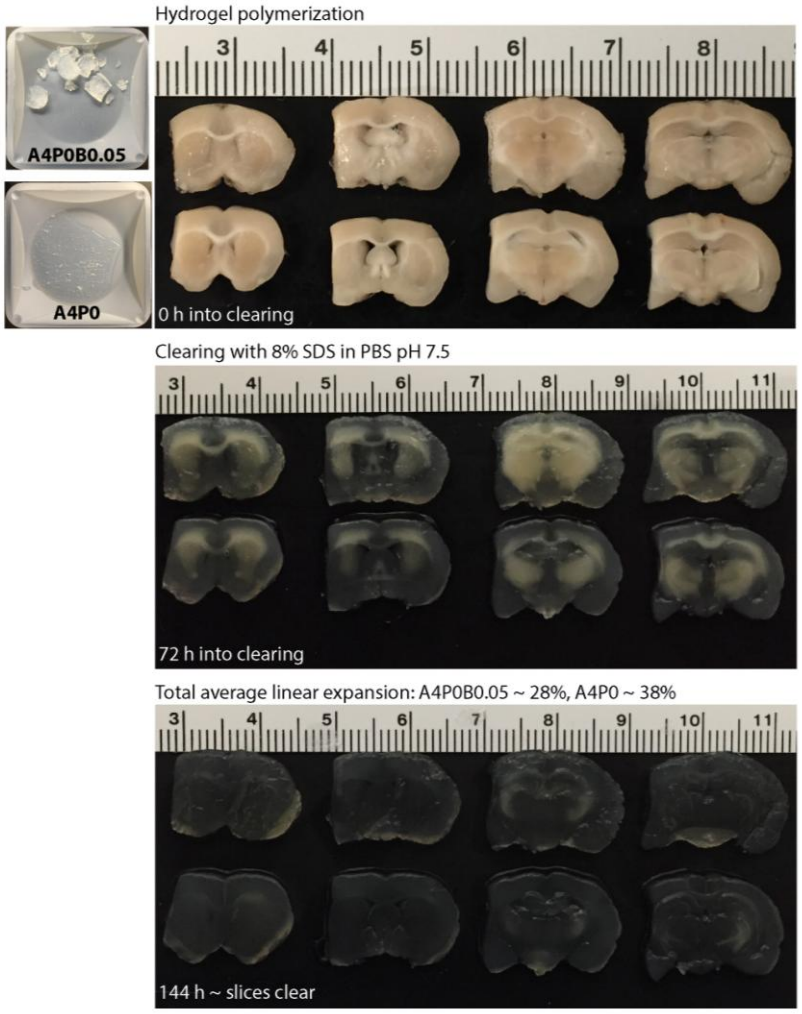

b **RIMS formulation guide to optimize the RIMS RI to that of the cleared sample**

Histodenz (g per 30 mL buffer)	RI	RIMS total volume (mL)	Histodenz (% wt/vol)
0	1.3330	30.00	0.0
5	1.3575	33.00	15.0
10	1.3790	36.00	28.0
15	1.3976	38.00	39.0
20	1.4134	39.50	51.0
25	1.4285	42.00	60.0
30	1.4413	45.00	67.0
35	1.4536	47.00	74.0
40	1.4655	48.75	82.0
42	1.4685	50.50	83.0
45	1.4741	52.00	87.0
47	1.4818	52.50	90.0
50	1.4849	53.00	94.0
55	1.4917	55.00	100.0

Treweek et al., 2015

Nature Protocols: doi:10.1038/nprot.2015.122

Supplementary Figure 1

Effects of bis-acrylamide crosslinker on clearing time and swelling of PACT-cleared sections.

(**a**) Representative images of the time course for PACT clearing of four 2 mm thick rat coronal brain slices, (displayed anterior to posterior, from left to right). Slices were embedded in either A4P0B0.05 or A4P0 and then cleared with 8% SDS-PBS (pH 7.5). The A4P0 slices were completely clear by 144 hours. Although some heavily myelinated brain sections seemed to resist clearing in A4P0B0.05-embedded sections initially, this effect did not persist, resulting in similar overall clearing time as slices embedded without bis-acrylamide. Likewise, tissue transparency was indistinguishable between conditions after their 48-hour incubation in RIMS. Unlike in 1 mm sections (Fig. 3), bis-acrylamide did limit tissue expansion in 2mm thick slices (A4P0: 38% total average linear expansion, A4P0B0.05: 28% average linear expansion). (**b**) RIMS formulation guide to optimize the RI to that of the cleared sample. RIMS formulated with 82% Histodenz^{TM} (RI = 1.4655) should be broadly applicable to cleared brain tissue, while RIMS with a higher RI of 1.48-1.49 (RIMS-1.48, RIMS-1.49) is suggested for denser cleared tissue such as bone (Fig. 6).

Figure S2

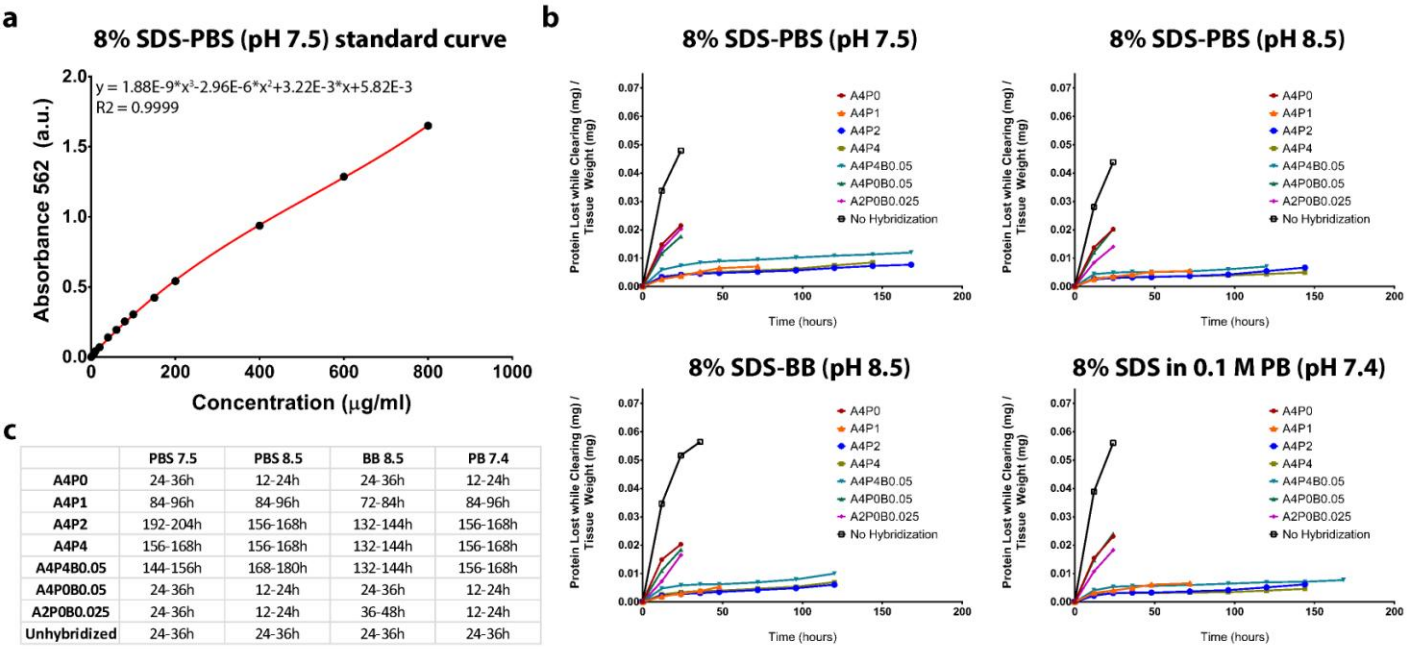

c

	PBS 7.5	PBS 8.5	BB 8.5	PB 7.4
A4P0	24-36h	12-24h	24-36h	12-24h
A4P1	84-96h	84-96h	72-84h	84-96h
A4P2	192-204h	156-168h	132-144h	156-168h
A4P4	156-168h	156-168h	132-144h	156-168h
A4P4B0.05	144-156h	168-180h	132-144h	156-168h
A4P0B0.05	24-36h	12-24h	24-36h	12-24h
A2P0B0.025	24-36h	12-24h	36-48h	12-24h
Unhybridized	24-36h	24-36h	24-36h	24-36h

Treweek et al., 2015

Supplementary Figure 2

Protein loss over the course of PACT clearing.

The amount of protein lost while clearing was measured by performing a BCA on the clearing buffer, which was collected and replaced periodically while 1 mm tissue samples were undergoing PACT. A standard curve of BSA protein concentration in each of the four different clearing buffers was generated. Standard curves were fit with a third order polynomial and used to extrapolate all protein loss measurements. (**a**) A representative case, in which the absorbance in arbitrary units (a.u.) of standard solutions at 562 nm is plotted against known BSA concentrations in 8% SDS-PBS (pH 7.5). (**b**) Graphs show single-trial, representative protein loss measurements for each hydrogel condition in each clearing buffer. Protein content was measured at 12 hours into clearing, at 24 hours, and then every 24 hours until the samples were clear, and normalized to the initial weight of the slice. Experiments were performed in triplicates, representative single trials for each combination are shown. (**c**) Time to clear for 1 mm sections PACT-processed with all hydrogel embedding and clearing buffer combinations (*n* = 3 for A4P1, A4P2 and Unhybridized. *n* = 4 for all others).

Figure S3

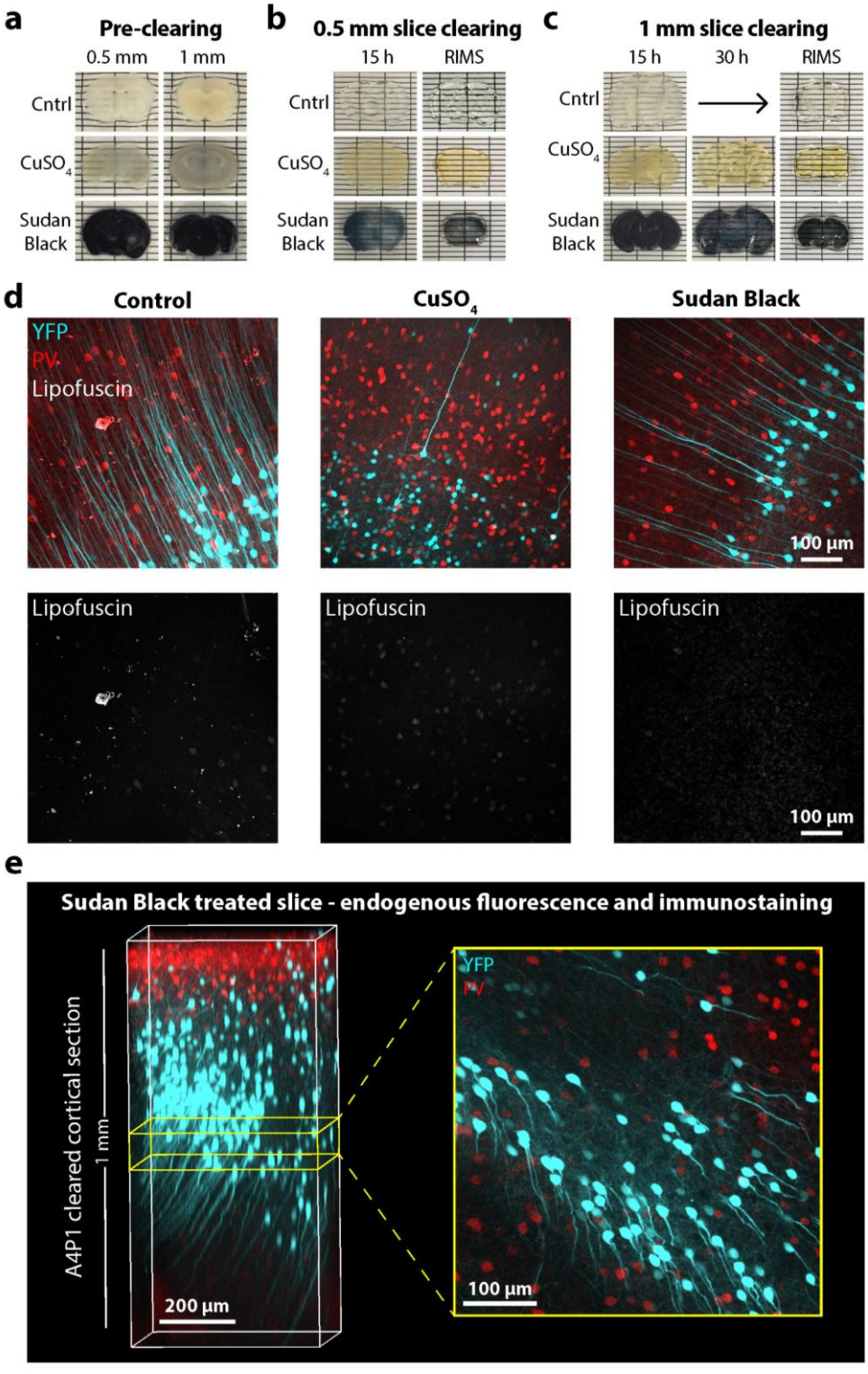

Treweek et al., 2015

Nature Protocols: doi:10.1038/nprot.2015.122

Supplementary Figure 3

PACT compatibility with histological staining.

(**a-c**) Representative images of thick section clearing with addition of $CuSO_4$ or 0.2% SB compared to regular PACT. 0.5 mm and 1 mm coronal Thy1-YFP mouse brain sections are shown after A4P1 hydrogel polymerization (**a**) and during clearing with 8% SDS-BB (pH 8.5) and subsequent 24 hour incubation in RIMS (**b** and **c** for 0.5 mm and 1 mm, respectively). (**d**) The control, $CuSO_4$, and 0.2% SB treated 0.5 mm slices from (**a-b**) were immunostained for parvalbumin (see Table 4) and then transferred to RIMS, degassed, and mounted. Shown are 500 μm thick maximum intensity projections of endogenous YFP (cyan) and parvalbumin (red) staining (top) as well as lipofuscin (white) autofluorescence (top and bottom). Red blood cell-derived (e.g. lipofuscin-like) autofluorescence was excited at 561 nm and collected between 562-606 nm. (**e**) Visualizing endogenous fluorescence and immunostaining deep within thick tissue. A 1 mm thick Thy1-YFP mouse brain coronal slice was treated with 0.2% SB, A4P1-embedded, cleared with 8% SDS-BB (pH 8.5), immunostained for parvalbumin (see Table 4), and then transferred to RIMS and mounted. Endogenous YFP (cyan) and immunolabeled PV (red) were imaged throughout the slice (left) in a region of the cortex. A 100 μm thick maximum intensity projection (right) was taken at a depth of 500 μm to show representative imaging in the middle of the section. Signal range of the red channel was adjusted for better visualization of PV staining at depth. All sections were imaged on a Zeiss LSM 780 confocal with the Plan-Apochromat 10× 0.45 N.A. M27 air objective (w.d. 2.0 mm).

Figure S4

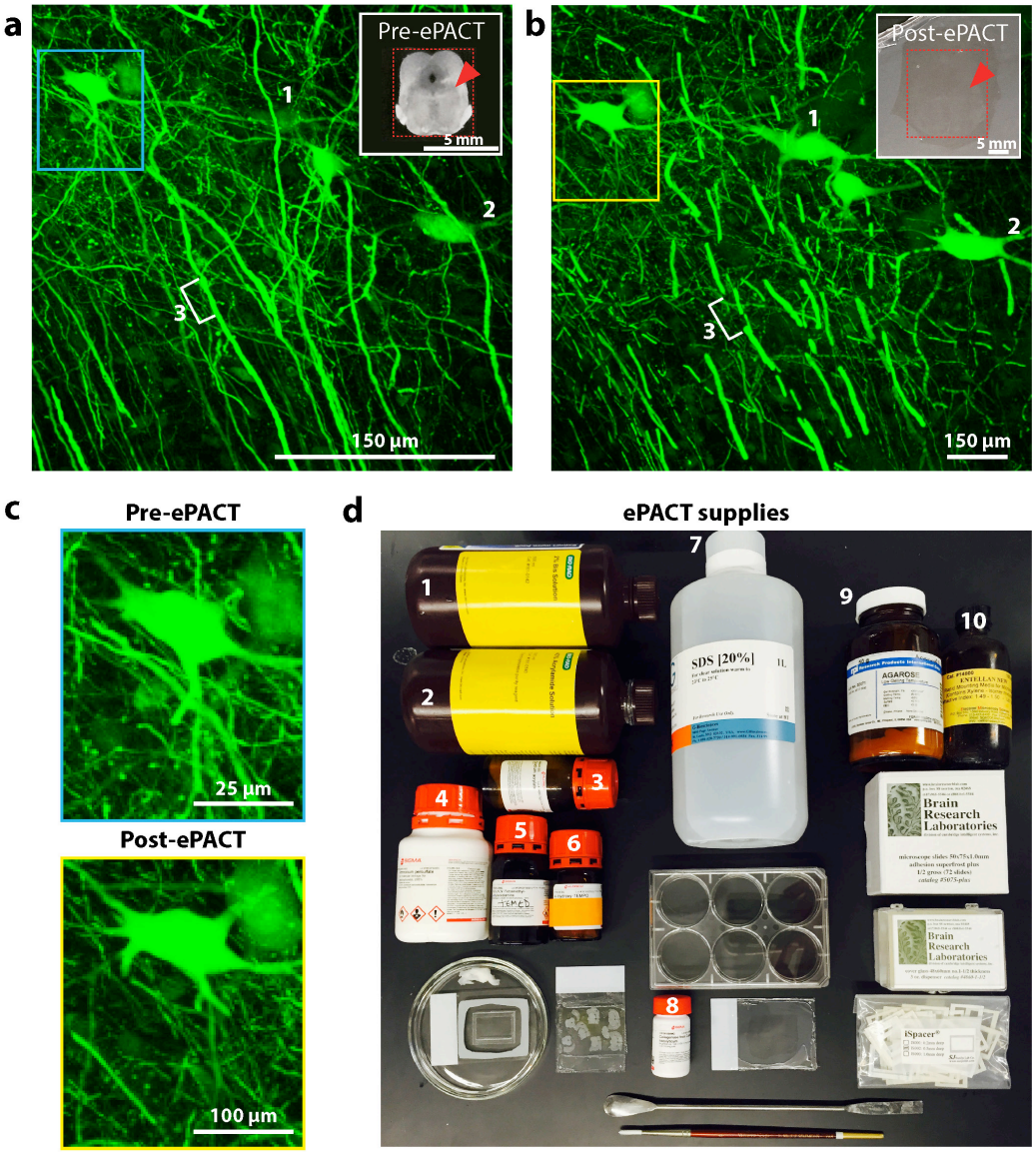

Treweek et al., 2015

Supplementary Figure 4

ePACT: a protocol for tissue clearing through expansion.

(**a**) Fluorescence image of Thy1-YFP expression prior to expansion-clearing. A 70 µm thick maximum intensity projection of five cells expressing YFP represents the standard for imaging pre-expansion. A bright-field image of the pre-expansion 100 µm brain slice is shown in the top right, with the location of the cells being imaged indicated by the red arrowhead. Noteworthy features that may differ between pre- and post- expansion-cleared tissue, such as cell bodies, branching processes, and large projections, are numbered 1, 2, and 3, respectively. (**b**) Fluorescence image of Thy-YFP expression after 4× expansion-clearing. A 340 µm thick

maximum intensity projection of the same five cells in (**a**) is shown, with the same features labeled again 1, 2, and 3. Of note, a cell body (1) and the neuronal processes of an adjacent cell (2) are both partially obstructed by tissue lipids in (**a**), but can be easily identified in (**b**) after clearing and expansion. However, the 4× expansion that contributes to this increased visibility through tissue also causes some tissue destruction, as apparent in the multiple severed processes, such as (3). A bright-field image of the expanded slice embedded in agarose is shown at the top right. (**c**) Native YFP fluorescence from the same cell in pre-expanded (blue box) and post-expanded (yellow box) tissue is shown. (**d**) Equipment for sample processing: (1) 2% bis-acrylamide, (2) 40% acrylamide, (3) sodium acrylate, (4) ammonium persulfate (APS), (5) N,N,N',N'-Tetramethylethylenediamine (TEMED), (6) 4-hydroxy TEMPO, (7) 20% SDS, (8) collagenase, (9) low gelling temperature agarose, (10) Entellan, and assorted, unlabeled, glass slides, spacers, and plastic dishes. All images were taken on a Zeiss LSM 780 confocal with the Plan-Apochromat 10× 0.45 N.A. M27 air objective (w.d. 2.0 mm).

Figure S5

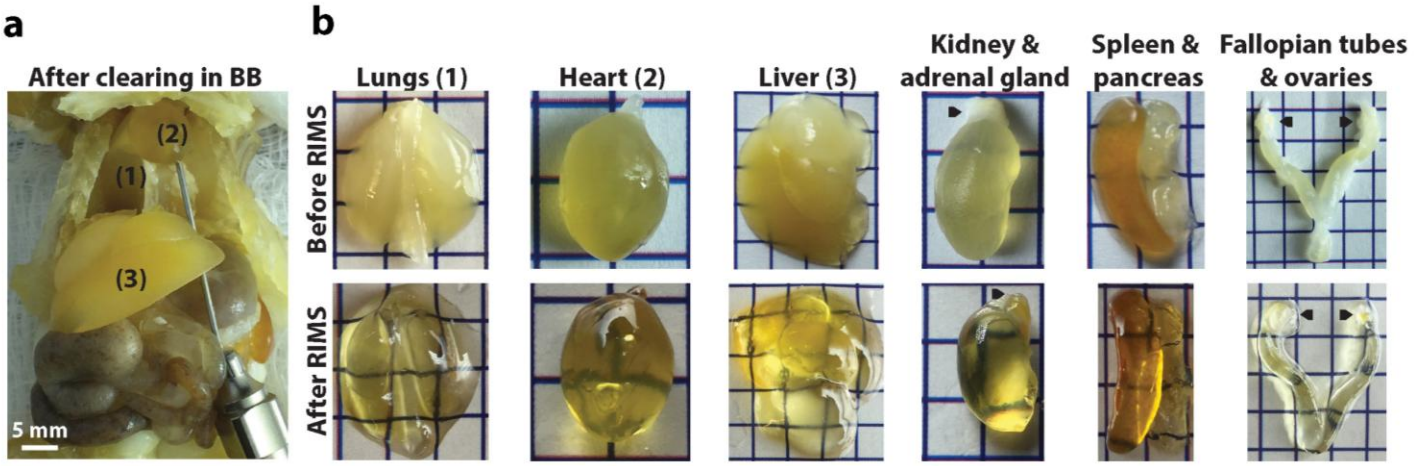

Treweek et al., 2015

Supplementary Figure 5

Whole body PARS clearing with borate-buffered detergent.

(**a**) Mice were perfusion-fixed, A4P0-embedded, PARS-cleared for 5 days with 8% SDS-BB (pH 8.5), and washed with 1× PBS at pH 7.5. Numbers correspond to the extracted organs in panel (**b**). (**b**) Extracted organs from the cleared mouse in panel (**a**), pictured before (top) and after (bottom) RIMS incubation for 3 days. Black arrowheads correspond to the adrenal gland on the kidney and to the ovaries on the fallopian tubes. Each square represents 0.5 cm^2. Rodent husbandry and euthanasia conformed to all relevant governmental and institutional regulations; animal protocols were approved by the Institutional Animal Care and Use Committee (IACUC) and by the Office of Laboratory Animal Resources at the California Institute of Technology.

Figure S6

a

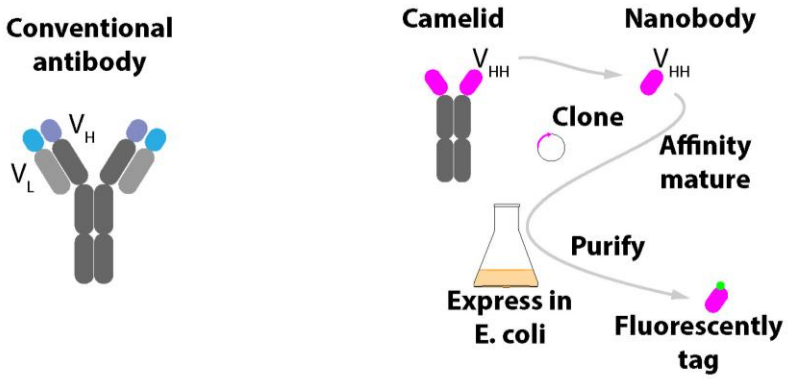

ANTIBODY	NANOBODY
150 kD, immunogenic	15 kD, weakly immunogenic
Slow tissue penetration	Rapid tissue penetration
Nano- to picomolar affinity	Nanomolar, rarely picomolar affinity
Risk of aggregation, denaturation	Stable at wide pH, temperature, salt ranges
Susceptible to degradation	Resistant to proteases
Expensive to obtain	Expensive to develop
Expansive, time-tested antibody selection	Limited current selection

b

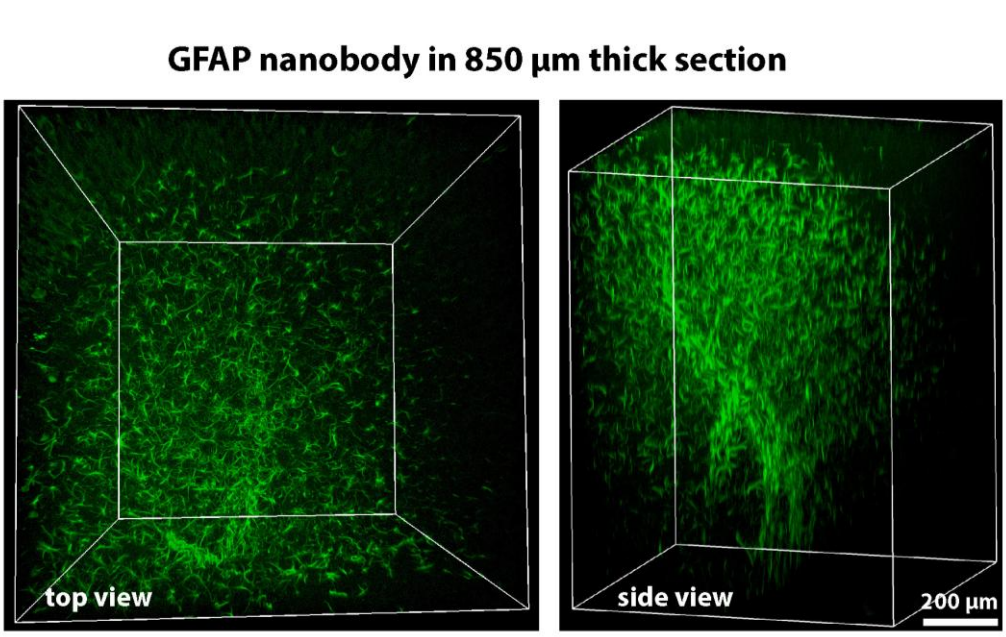

Treweek et al., 2015

Supplementary Figure 6

Small-format antibodies for thick-tissue labeling.

(**a**) For labeling thick tissue sections, camelid nanobodies are a promising alternative to traditional antibodies, either full immunoglobulins or their engineered formats (single-chain variable fragment (scFv), Fab, and $F(ab')_2$). A possible workflow for nanobody production consists of: inoculating 500 ml terrific broth with 5 ml overnight cultures and grow at 37 °C until IPTG induction at OD = 0.5, then lowering the temperature to 20 °C for 10 hours for nanobody expression. Cell pellets are then lysed, carried through alternating cycles of freeze-thaw with benzonase addition, followed by a final addition of 0.1% polyethyleneimine to the pellet lysate before pelleting debris and filtering the nanobody-containing fraction. The His-tagged GFAP fusion protein is purified by immobilized metal affinity chromatography on a Ni-NTA column. The His-tag must be removed prior to staining to avoid non-specific binding. (**b**) To stain for glial fibrillary acidic protein (GFAP) using a GFAP camelid nanobody, 1 mm thick PACT-cleared mouse brain sections were immunostained with 1:500 Atto 488 conjugated GFAP nanobody (see Table 4) at RT overnight with shaking. The stained sections were then washed 3 times in PBST over 1 hour, followed by a 1-hour incubation in RIMS. The transparent sections were RIMS-mounted and imaged on a Zeiss LSM 780 confocal with the Plan-Apochromat 10× 0.45 N.A. M27 air objective (w.d. 2.0 mm). (**b**, left) 850 μm thick 3D rendering of mouse internal capsule stained with GFAP nanobody. (**b**, right) Side view showing uniform labeling of GFAP nanobody throughout the entire 850 μm slice.

Figure S7

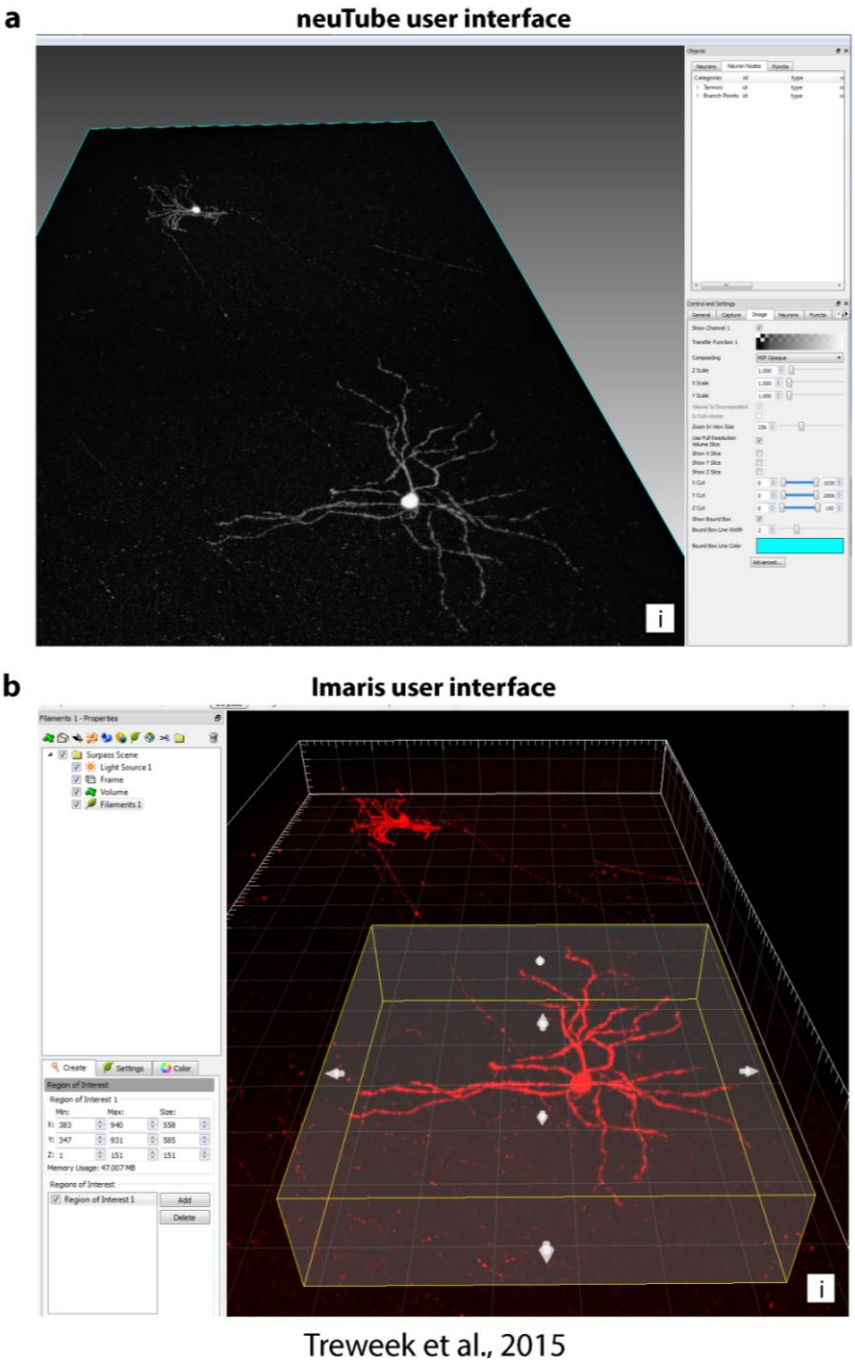

Supplementary Figure 7

User interface elements for image analysis.

(**a**) neuTube. (**b**) Imaris. Computer screenshots depict the image processing workspace for each software during the 3D visualization (i) of labeled cells in Figure 10.

Supplementary Methods
Nature Protocols
Treweek *et al*., 2015

AAV9 tropism studies

Figure 1a-e

1×10^{12} vector genomes of AAV9:CAG-GFP-2A-Luc-WPRE-SV40 late poly A (AAV9:CAG-GFP) was administered systemically (via retro-orbital injection) to 6-week-old female C57Bl/6 mice. Three weeks later, mice were perfused and cleared via PARS, and individual organs were harvested and equilibrated in RIMS until clear (up to 7 days) before mounting in fresh RIMS and imaging.

Experiments on vertebrates must conform to all relevant governmental and institutional regulations. Animal husbandry and all experimental procedures involving mice and rats were approved by the Institutional Animal Care and Use Committee (IACUC) and by the Office of Laboratory Animal Resources at the California Institute of Technology.

Quantification of Ab penetration through PACT-cleared tissues

Figure 4b-d

Mouse coronal slices, 1 mm thick cleared with PACT conditions as stated and stained with anti-parvalbumin antibody and DAPI, were used to analyze the rate of diffusion of antibodies and small molecule dyes through cleared tissue. A column through the depth of the tissue was imaged on a Zeiss LSM 780 confocal with the Plan-Apochromat 10× 0.45 N.A. M27 air objective (w.d 2.0 mm). Measured image intensities in each channel for each z-section were scaled to correct for varying laser power and yield an estimate of fluorescence. Image stacks were manually cropped (in z) to include only the “upper half” of the tissue section nearest the imaging objective and (in xy) to exclude areas where the top tissue surface was curved, an effect sometimes observed as tissue expands while clearing.

Quantitative image analysis was carried out using a custom MATLAB script. To factor out attenuation loss along the z-axis and account for varying cell density, the antibody fluorescence signal was scaled by the average DAPI intensity and computed perpendicular to the tissue surface to estimate labelling intensity as a function of depth. To fit this signal, we first identified the location

Nature Protocols: doi:10.1038/nprot.2015.122

of the surface as the point of maximum staining level and the center of the section as the point of minimum staining level. Since the surface is not perfectly flat, we excluded the top 20 μm above the maximum point of the signal from further analysis. Data points plotted in Figure 4d show the staining level starting 20 μm below the maximum down to the minimum staining level.

To provide a quantitative estimate of diffusion, we fit an exponential model (appropriate for idealized steady state of diffusion-decay into an infinite half-space with fixed boundary concentration) with an additive term to account for background fluorescence:

$$f(x) = a * \exp(-tau*x) + b$$

where the exponent tau is inversely proportional to the square-root of the diffusivity (i.e. a larger tau implies slower diffusion). If the staining level followed this model we would expect to see linear decay with depth on the semi-log plots shown in Figure 4d. We observe that staining levels near the surface of the tissue fall below an exponential model (likely due to post stain washing). Similarly, signal near the center of the tissue, where staining is ~1% the level observed on the surface, is noisy (e.g., due to imaging noise, stochastic fluctuations at low concentration, not reaching steady state). Therefore we used staining level between 20% and 80% depth to fit the exponential model (this range is indicated by the extent of the straight lines for each sample shown in Fig. 4d).

Cleared tissue preparation for electron microscopy and tomography
Figure 5b

BACKGROUND

To incorporate high-resolution, subcellular information into lower-resolution tissue maps requires performing correlative studies between light microscopy (LM) and electron microscopy (EM) datasets. While the tandem preparation of individual thin tissue slices for both LM and EM analysis is relatively commonplace, not until recently have scientists envisioned applying this approach to a large spatial extent, such as whole organs[1-8]. Despite the obvious challenge in reconstructing tissue architecture from nanoscale tiles, this is currently the only viable method for creating comprehensive wiring diagrams[9-11]. Neither light-microscopic observations nor the (statistical extrapolation) mathematical inference of cellular connectivity can provide high-resolution circuit maps with sufficient statistical certainty[12]. Instead, cellular structures and synaptic contacts must be visualized first-hand in order to create valid tissue reconstructions.

Herein, one could envision a cell-mapping methodology in which large tissue blocks were first scanned via LM, and then sub-sectioned for EM analysis. While the former is easily completed

Nature Protocols: doi:10.1038/nprot.2015.122

by imaging through cleared tissue blocks, the latter faces a few technical challenges. Namely, lipid-extracted tissues make poor subjects for high-resolution EM studies. A fundamental component of tissue clearing, delipidation compromises the structural integrity of remaining subcellular constituents and eliminates a primary source of ultrastructural contrast in EM (i.e., osmium tetroxide based fixation-staining of lipids, and thus of all cell membranes and membrane-enclosed organelles). Without this contrast, the process of identifying fine structures or tracing cellular elements between images, assuming they survive clearing, becomes problematic.

A second concern in the translation of cleared tissues to EM is their method of preparation. Traditionally, tissue that is slated for ultrastructural analysis undergoes a highly regimented fixation, freeze-substitution, and/or immunostaining process to ensure that the subcellular architecture is well-preserved for high-resolution visualization and reliable immunolocalization. The tissue clearing procedure departs from standard EM methods even at its onset: tissues are initially fixed in 4% PFA with no inclusion of glutaraldehyde, a staple in EM fixatives. Similarly, extended incubations at room temperature (RT) to 37 °C in solutions where pH and osmolarity are imprecisely controlled, are suboptimal conditions for the preservation of fine structures.

Cognizant of these impediments, we hypothesized that ultrastructural analysis of cleared tissue samples through transmission electron microscopy (TEM) would still provide relevant data on the degree of lipid extraction within different samples. By comparing the fine structural preservation in control, A4P0-embedded, and A4P4-embedded tissues, we might make inferences on slight difference in clearing efficiency and hydrogel-based retention of tissue components that are not readily apparent by eye or by LM.

EXPERIMENTAL METHODS

Brain tissue samples from each of the clearing conditions were processed simultaneously for subcellular examination via electron tomography[13]. Each sample was placed in a petri dish containing 0.1 M sodium cacodylate trihydrate + 5% sucrose. Similar regions were extracted from each sample and cut into 0.50-0.75 mm cubes. These pieces were placed into a brass planchette (Ted Pella, Inc.) prefilled with cacodylate buffer supplemented with 10% Ficoll (70kD; Sigma-Aldrich) which serves as an extracellular cryoprotectant. The sample was covered with second brass planchette and rapidly frozen with a HPM-010 high-pressure freezer (Leica Microsystems, Vienna), then stored in liquid nitrogen.

Planchettes containing vitrified samples were transferred under liquid nitrogen to cryotubes (Nunc) filled with 2.5% osmium tetroxide, 0.05% uranyl acetate in acetone. Tubes were placed into an AFS-2 freeze-substitution machine (Leica Microsystems) and processed at -90 °C for 48 hours,

Nature Protocols: doi:10.1038/nprot.2015.122

warmed slowly over 12 hours to -20 °C and further processed at that temperature for 10 hours. The tubes were then warmed to 4 °C for 1 hour and the samples rinsed 4× with cold acetone. Samples were removed from the planchettes, infiltrated into Epon-Araldite resin (Electron Microscopy Sciences, Port Washington PA) and flat-embedded between two Teflon-coated glass microscope slides.

Embedded samples were observed with a phase-contrast light microscope and similar portions from each condition was extracted and glued to plastic sectioning stubs. Semi-thick sections (350 nm) were cut with a UC6 ultramicrotome (Leica Microsystems) and a diamond knife (Diatome-US, Port Washington PA). Sections were placed on Formvar-coated copper/rhodium slot grids (Electron Microscopy Sciences) and stained with 3% uranyl acetate and lead citrate. Colloidal gold particles (10 nm) were placed on both sides of the grid to serve as fiducial markers for tomographic image alignment. Grids were placed in a 2040 dual-axis tomography holder (E.A. Fischione Instruments, Inc., Export PA) and imaged with a TF30-ST electron microscope at 300KeV. Montaged overviews and tomographic tilt-series were acquired automatically using the Serial-EM software package[14]. Samples were tilted +/- 64° and 2k × 2k images recorded at 1° intervals with a XP1000 CCD camera (Gatan, Ltd.). Image data was processed and analyzed using the IMOD software package[15] on a MacPro computer (Apple, Inc.).

ANTICIPATED RESULTS

The control sample of this experiment was fixed only by 4% PFA perfusion, akin to cleared samples, and then processed for TEM. Its retention of fine structure was readily apparent (see Fig. 5b, Control), and the level of gross tissue damage was minimal considering the nontraditional method of preparation. Significantly less fine structure was discernable in the cleared samples, as was predicted, and the lipid-containing membranes were fully solubilized or highly ruptured. Of note, the addition of paraformaldehyde to hydrogel formulations served to attenuate lipid extraction and led to greater preservation of neuronal processes (see Fig. 5b, A4P4).

These results highlight the potential for incorporating EM analysis into tissue clearing and LM experiments. A modified perfusion followed by a more aggressive post fixation and/or freeze-substitution might offer some ultrastructural stabilization that persists through clearing. Herein, it would be possible to carry uncleared control samples through to high-resolution tomographic studies, while matched samples were processed for clearing and LM.

Nature Protocols: doi:10.1038/nprot.2015.122

Pre-PACT tissue staining to mask autofluorescence
Figure S3

BACKGROUND

The following protocol summarizes how tissue stains used in traditional histology, and in particular, stains used to quench lipofuscin-derived fluorescent artifacts, may be incorporated into the PACT protocol. Representative results are presented in Figure S3.

Autofluorescent artifacts and high background pose a greater threat to imaging through thick tissue than through thin as they significantly decrease the signal-to-noise ratio, making the distinction between specific labeling and nonspecific autofluorescence difficult. Among the most common causes of autofluorescence in tissue are tissue-aldehyde adducts from aldehyde-based fixatives and catecholamine, collagen, elastin, the heme chromophore, and degradation products of red blood cells (i.e., the lipid peroxidation and protein glycation aggregates, such as lipofuscin, that can accumulate in aging red blood cells)[16]. For biological researchers, the latter source of autofluorescence becomes a major concern when working with tissue samples from aged subjects (e.g., old laboratory animals) or with poorly perfused, overfixed samples (e.g. post-mortem or biopsied human tissue). Herein, a few tissue stains, most notably Sudan Black B and cupric sulfate, have been found to mask lipofuscin-like autofluorescence in the histological preparation of thin-sectioned (< 0.5 mm) tissues[17-19]. Thus, we endeavored to test their compatibility with thick, PACT-cleared rodent brain sections (see Fig. S3) according to the experimental methods detailed below.

REAGENTS

- Perfusion-fixed (4% PFA) 0.5-1 mm coronal brain slices from Thy1-YFP mice
- Sudan Black B (Sigma-Aldrich, cat. no. 199664)
- Ethanol (Sigma-Aldrich, cat. no. E7023; or Fischer Scientific, cat. no. BP2818)
- Cupric Sulfate (Fisher Scientific, cat. no. S25285A)
- Ammonium Acetate (Sigma-Aldrich, cat. no. A1542)
- PACT Hydrogel Monomer (HM) solution (A4P1)
- PACT Clearing solution: 8% SDS-BB (pH 8.5)
- Optional: PACT IHC reagents and IHC buffer
- Refractive Index Matching Solution (RIMS, RI = 1.47)
- 1× Phosphate-buffered saline (1× PBS), pH 7.4
- 1× PBS with 0.1% (vol/vol) Triton X-100 (PBST)

Nature Protocols: doi:10.1038/nprot.2015.122

- 0.1 M Phosphate buffer (PB), pH 7.4
- Sodium azide (Fisher Scientific, cat. no. 71448-16)
- Distilled and deionized water (dd H_20)

EQUIPMENT

- Syringe filters (Corning, cat. no. CLS431218)
- 30 ml Luer-Lok syringes (BD, cat. no. 302832)
- Hydrogel polymerization equipment and supplies
- PACT equipment and supplies
- Sample mounting equipment and supplies

REAGENT SET-UP

- Cupric sulfate lipofuscin treatment ($CuSO_4$): Prepare 10 mM cupric sulfate in 50 mM ammonium acetate (CH_3COONH_4) buffer; adjust the pH = 5.0.
- Sudan Black B lipofuscin treatment (SB): Prepare 0.2% Sudan Black B in 70% ethanol in a sealable container or jar; protect from light. Alternatively, if tissue possesses a high level of lipofuscin, or if tissue will undergo extensive immunolabeling, which can wash off SB staining, prepare 1% SB in 70% ethanol. With the container sealed and wrapped in tin foil, stir the SB solution on a stir-plate at high-speed for 2 hours (or up to overnight). Syringe-filter the SB solution two times and use immediately.

EXPERIMENTAL METHODS

Thy1-YFP mice were perfusion-fixed with 4% PFA, and the excised brains were cut into 0.5 mm and 1 mm coronal sections. Upon brief post-fixation, sections were rinsed in 1× PBS and then dd H_2O, and then incubated in either 1× PBS (control), 10 mM $CuSO_4$, 0.2% SB, or 1% SB for 2-3 hours at RT with shaking[17]. Sections were then dipped in dd H_2O to remove excess stain, briefly rinsed in 1× PBS, and incubated in A4P1 for 48 hours at 4 °C before hydrogel polymerization according to standard PACT procedures. $CuSO_4$ but not SB seemed to interfere with polymerization, as the hydrogel did not fully set. A4P1 sections (see Fig. S3a) were then cleared in 8% SDS-BB (pH 8.5), with all 0.5 mm sections (see Fig. S3b) and the control 1 mm section (see Fig. S3c) becoming translucent after ~ 12-15 hours. The $CuSO_4$-treated and SB-treated 1 mm sections required an increased (~24-48 hours) time to clear in comparison to the control (see Fig. S3c). All sections were immunostained for parvalbumin (Cy5-conjugated secondary IgG) according to the standard PACT IHC protocol and transferred to RIMS for 24 hours (see Fig. S3b-c), followed

Nature Protocols: doi:10.1038/nprot.2015.122

by degassing and RIMS-mounting. 0.5 mm thick sections were imaged on a Zeiss LSM 780 confocal with the Plan-Apochromat 10× 0.45 N.A. M27 air objective (w.d 2.0 mm) to independently measure the emission profiles generated by excitation with the 561 nm laser (filter bandpass for rhodamine/Cy3) versus by the 488 nm and 633 nm lasers, using filters for YFP and Cy5 fluorescence, respectively.

ANTICIPATED RESULTS

In these experiments, we aimed to assess whether SB or $CuSO_4$ tissue pretreatment could reduce autofluorescent background in brain tissue without masking endogenous fluorescent proteins and immunofluorescent labels (YFP, Cy5-conjugateded secondary antibody). The emission spectra generated by the YFP and Cy5 fluorophores were compared to the autofluorescence spectra within the orange to red wavelengths (rhodamine/Cy3 filter), where the absence of any specific labeling would allow us to clearly observe fluorescent artifacts. The resulting imaging data, which are presented as 500 μm thick maximum intensity projections (MIP) over the cortex for each treatment condition (see Fig. S3d, top row), demonstrate that neither SB nor $CuSO_4$ treatments prevented the visualization of YFP and Cy5 fluorophores (and DAPI, data not shown) in thick cleared sections. Both treatments were effective in reducing autofluorescent background and masking the fluorescence of lipofuscin-like deposits, as shown in the duplicate MIPs for the fluorescence emission collected using the rhodamine/Cy3 bandpass filter (see Fig. S3d, bottom row).

To investigate whether the potential for deep imaging was retained after 0.2% SB treatment (see Fig. S3c), a 1.0 mm thick section was imaged for YFP and Cy5 fluorescence through its entire thickness within a cortical region (see Fig. S3e, left), and a 100 μm thick MIP (see Fig. S3e, right) was generated in order to display the endogenous fluorescence and staining that is visible at depth. While endogenous YFP fluorescence is very bright and of almost uniform intensity throughout the slice, which speaks to the efficacy of PACT clearing in A4P1-embedded slices, immunolabeling intensity suffers at depth, and requires adjustment of signal intensity or laser power for visualization.

Nature Protocols: doi:10.1038/nprot.2015.122

ePACT: a protocol for enhanced clearing via expansion

Figure S4

BACKGROUND

The following protocol, termed ePACT for expansion-enhanced PACT, details the experimental methods used to prepare the cleared and expanded brain sections pictured in Figure S4.

REAGENTS

- Perfusion-fixed 100 µm rodent brain slices
- (optional) PACT IHC reagents
- 40% Acrylamide (40% wt/vol; Bio-Rad, cat. no. 161-0140)
- 2% Bis-acrylamide (2% wt/vol; Bio-Rad, cat. no. 161-0142)
- Sodium acrylate (Sigma-Aldrich, cat. no. 408220)
- Sodium chloride (NaCl) (Sigma-Aldrich, cat. no. S5886)
- 1× PBS
- 4-hydroxy TEMPO (Sigma-Aldrich, cat. no. 176141)
- N,N,N',N'-Tetramethylethylenediamine (TEMED, Sigma-Aldrich, cat. no. T9281)
- Ammonium persulfate (APS, Sigma-Aldrich, cat. no. A1542)
- Boric acid (Sigma-Aldrich, cat. no. B7901 or B6768)
- Sodium hydroxide pellets (EMD, cat. no. SX0590-3)
- Sodium dodecyl sulfate (Sigma-Aldrich, cat. no. L3771) or 20% SDS solution in water (Sigma-Aldrich, cat. no. 05030)
- 10× PBS
- Collagenase, crude from *Clostridium histolyticu*m (Sigma-Aldrich, cat. no. C0130)
- Calcium chloride (Sigma-Aldrich, cat. no. C1016)
- TES (Sigma-Aldrich, cat. no. T5691)
- distilled/deionized water (dd H_2O)
- Agarose, low melt temperature (Research Products International Corp., cat. no. 9012-36-6)
- Sodium azide (Fisher Scientific, cat. no. 71448-16)
- Clear nail polish or Entellan (Electron Microscopy Sciences, cat. no. 14800)

EQUIPMENT

Nature Protocols: doi:10.1038/nprot.2015.122

- For hydrogel-embedding: 0.2 mm and 0.5 mm spacers (iSpacer, SunJin Lab Co, cat. no. IS001, IS002), or HybriWell™ Sealing System (GRACE Bio-Labs, cat. no. 611103, 611104, 612106 (select based on sample size and number))
- (optional) Spacers for enzymatic digestion and/or mounting, order based on sample size): 0.5 mm or 2.5 mm spacers (Silicone Isolator, Electron Microscopy Sciences; or GRACE Bio-Labs), or silicone rubber sheet (any, such as: Press-to-Seal™ Silicone Sheet with Adhesive, Fischer Scientific, cat. no. P-24745)
- Clear nail polish or Entellan (Electron Microscopy Sciences, cat. no. 14800)
- Microscope slides (Thermo Scientific, cat. no. 10143352; VWR, cat. no. 48382-173; Brain Research Laboratories, cat. no. 5075-plus)
- Cover slips (VWR, cat. no. 48404-452, 16004-344, 16004-322; Brain Research Laboratories, cat. no. 4860-1-1/2)
- ePACT sample washing and clearing wells, such as 6-well tissue culture plates and/or petri dish
- Slide humidifier (we use a petri dish with lid containing a moistened Kimwipe)
- 37 °C incubator or warm-room, with a nutating mixer inside
- Tools for sample handling (forceps, natural-bristle paintbrush, tweezers: Fine Science Tools; lab spoons, spatulas: any, such as Sigma-Aldrich, cat. no. Z511455)
- Eppendorf tubes (0.5, 1.5, 2.0 ml volumes)

REAGENT SET-UP

- **ePACT acrylate-acrylamide copolymer (AcAm)**: Combine 2.5% acrylamide, 8.625% sodium acrylate, 0.15% bis-acrylamide in 1× PBS with 2 M NaCl; store at -20 °C prior to use. For tissue embedding, thaw AcAm on ice, and add the following (w/w): 0.01% 4-hydroxy TEMPO, 0.2% TEMED, and 0.2% APS (see Fig. S4d)
- **0.01 M Phosphate-buffered saline (PBS)**: Combine 8g NaCl, 0.2g KCl, 1.42g Na_2HPO_4, 0.245g KH_2PO_4 in distilled H_2O (dH_2O) to a total volume of 1 L; pH to 7.4, sterile filter or autoclave, and store at 4 °C. Alternatively, purchase 1× PBS mix (Sigma Aldrich, cat. no. P5368) or pre-made solution (Lonza, cat. no. 04-409R) from a commercial supplier; adjust the final pH when necessary.
- **Boric acid buffer (BB)**: Prepare a 1 M boric acid buffer stock solution through stirring 61.83 g boric acid and 10 g NaOH in 900 ml water with gentle heating. Once sodium hydroxide pellets and boric acid are fully dissolved, adjust the pH to 8.5 with NaOH and add distilled and deionized water (dd H_2O) to a total volume of 1 L. Dissolve this stock 5-fold for

Nature Protocols: doi:10.1038/nprot.2015.122

0.2 M boric acid buffer (BB). To make a boric acid wash buffer (BBT, 0.2 M boric acid buffer with 0.1% Triton X-100 (vol/vol), pH 8.5), dilute the 1 M boric acid stock to 0.2 M boric acid in dd H_2O, adding 1 ml of Triton X-100 per litre of BBT.

- **ePACT clearing solution**: For borate-buffered 10% SDS in 0.2 M BB at pH 8.5 (10% SDS-BB), dilute 500 ml 20% SDS and 200 ml 1 M boric acid buffer stock to 1 L with dd H_2O; adjust the pH to 8.5, if necessary.
- **TESCA buffer**: Prepare 50 mM TES, 0.36 mM Calcium chloride solution, pH 7.4; sterile filter and store at RT.
- **ePACT digestion solution**: 10 mg/mL collagenase in TESCA buffer, prepared fresh
- **Mounting media**: 2% low-melt agarose. Expanded samples may be stored at RT for ~ 72 hours prior to imaging if 0.01% sodium azide is added to the melted agarose solution immediately prior to pouring, and if the cover-slipped sample is sealed with Entellan.

PROCEDURE

CRITICAL The following steps have been optimized for clearing and expanding 100 µm thick rodent brain slices (from wild type rats, Thy1-YFP mice). To perform IHC with full-format antibodies prior to clearing, the tissue must be thoroughly permeabilized to obtain the best results. We suggest freezing in OCT medium, cryotome-sectioning to 100 µm, and performing IHC on free-floating sections according to standard protocols. Alternatively, the post-fixed mouse whole-brain may be vibratome-sectioned to 100 µm thick slices and permeabilized with ≤ 1% Triton X-100 (1 hour, RT with shaking). Without freeze-thaw permeabilization, antibody labeling may be weaker, and one may encounter difficulties expanding larger tissue samples (e.g., coronal rat brain slices) several-fold without some tissue damage.

Sample Preparation

1 Perfusion-fix the rodent with 4% PFA; excise and post-fix the brain overnight.

2 Prepare 100 µm thick tissue samples via sectioning on cryotome (option A, recommended for most samples) or on vibratome (option B, recommended for rapid visualization of endogenously-labeled small samples such as mouse coronal brain sections).

(A) Sample Preparation via Cryotome-sectioning

(i) Cryoprotect the sample in 30% sucrose at 4 °C with shaking; incubate until the sample sinks.

(ii) Tissue-off the sample, submerge the sample in OCT medium for < 5 minutes in a plastic tissue mold, and then snap-freeze in an isopentane-dry ice slurry.

Nature Protocols: doi:10.1038/nprot.2015.122

PAUSE POINT The sample may be stored at -80 °C for up to a few months.

(iii) Cryotome-cut the frozen sample, collecting sections in PB.

(iv) Thaw and rehydrate free-floating sections in PB for 20 min at RT to remove OCT medium.

(v) Permeabilize sections for 1 hour at RT in PBST containing 0.1%-1.0% Triton X-100 and 100 mM glycine; then, rinse in 1× PBS.

PAUSE POINT Sections may be stored at 4 °C in 1× PBS with 0.01% sodium azide for ≤ 1 day.

(B) Sample Preparation via Vibratome-sectioning

(i) Cut 100 µm thick tissue sections on the vibratome according to manufacturer's instructions.

(ii) Collect sections free-floating into 1× PBS.

(iii) Permeabilize sections for 1-2 hours at RT in PBST containing 0.1%-1.0% Triton X-100 and 100 mM glycine; then, rinse in 1× PBS.

PAUSE POINT Sections may be stored at 4 °C in 1× PBS with 0.01% sodium azide for ≤ 1 day.

3 (Optional) Label free-floating tissue sections according to standard IHC protocols. Antibody incubations should be conducted for 24 hours at 4 °C. Perform wash steps in PBST. The final wash should be conducted in 1× PBS.

4 (Optional) Image the pre-expanded sample. The section may be mounted on a non-treated glass slide in PB in order to visualize gross tissue morphology and, if applicable fluorescent signal strength. For finer visualization, incubate the section in RIMS for 1-2 hours prior to imaging. After imaging, wash RIMS-infused samples in 1× PBS (3 × 15 minutes).

ePACT Hydrogel Embedding

5 Thaw ~ 400 µl AcAm per 1 rat brain section or per 2 mouse brain sections. Add 4-hydroxy TEMPO, TEMED, and APS to half the thawed AcAm in an Eppendorf tube(s) on ice.

6 Immediately transfer the tissue sections into the Eppendorf tube(s) using a paintbrush. Tap the tube(s) to mix, ensuring that the samples are fully submerged in AcAm, and incubate at 4 °C with gentle shaking for 20-30 minutes (depending on the sample size).

7 Place a prepared slide (with a 0.2 mm iSpacer well, or similar alternative) in a petri-dish humidifier (see Fig. S4d, lower left) and pre-chill at 4 °C.

8 Add 4-hydroxy TEMPO, TEMED, and APS to the second half of the thawed AcAm in an Eppendorf tube(s) on ice.

9 Transfer the tissues by paintbrush from the Eppendorf to the chilled slide. Pipette the fresh AcAm solution onto the tissues in the iSpacer well, and smooth out the tissues, removing

Nature Protocols: doi:10.1038/nprot.2015.122

any bubbles that form. Coverslip, and return the sample + petri-dish humidifier to 4 °C for an additional 20-30 minutes.

10 Then, incubate the sample + petri-dish humidifier at 37 °C until the AcAm gel has polymerized (2-4 hours). Ensure that the Kimwipe in the humidifier stays moist during this incubation.

11 (Optional) The AcAm-embedded and polymerized sample may be imaged while it is thus mounted before continuing on to step 12.

ePACT Tissue Clearing

12 Using a razor blade or scalpel, cut around the tissue-hydrogel and carefully remove excess gel.

CRITICAL STEP It is crucial that extra gel be removed or the expanded tissue is very difficult to handle. Slice around the outline of the tissue with the scalpel blade, and carefully roll away the excess gel with a paintbrush. Do not try to remove gel from the flat surface of the brain.

13 Now, carefully remove the AcAm-embedded sample from the slide, and transfer to a sample dish containing 10% SDS-BB (pH 8.5).

CRITICAL STEP It is crucial to handle the tissue with care. Pipette ~ 0.5 ml clearing buffer onto the sample, and gently slide the paintbrush bristles between the glass slide and sample in order to loosen the AcAm gel's adhesion to the slide. Then, use a spatula to transfer the section between the slide and clearing dish.

14 Clear the tissue overnight at 37 °C with gentle shaking (i.e. on an orbital shaker or nutating mixer placed inside a 37 °C incubator or warm room).

15 Once clear, rinse the sample in BBT and then TESCA buffer for 1-5 minutes each at 37 °C. We have found that 6-well plates work well for this process. The tissue may be cleared in ~ 5 ml 10% SDS-BB (pH 8.5) in the first well, and the next day, transferred into the adjacent well for washing in 5ml BBT, and then transferred to the adjacent third well for washing in TESCA buffer.

16 Digest the sample in 10 mg/ml collagenase in TESCA buffer for 12-24 hours (i.e. all day for small samples, or all-day and overnight).

CRITICAL STEP The tissue should be fully saturated in digestion buffer, however to conserve reagents, it is not necessary to fully submerge the tissue in excess collagenase solution. Small sections (mouse coronal slices) may be transferred back into an iSpacer well (0.5-1 mm) for digestion; coverslip the sample and digest in a petri dish humidifier at 37 °C, as in steps 9-10. Larger sections (rat coronal slices) require more space. Transfer these sections into a clean well

Nature Protocols: doi:10.1038/nprot.2015.122

of a 6-well plate, saturate in digestion buffer (~ 0.5 ml), parafilm-seal the well/plate, and digest at 37 °C. Alternatively, samples may be digested within a larger sample well cut from a silicon matte and adhered onto a slide (see Fig. S4d); coverslip and digest within a petri dish humidifier at 37 °C.

Expansion-based Clearing

17 Soak the digested tissue in dd H_2O. This may be accomplished via placing a large, clean slide on the bottom of the petri dish, transferring the section onto the slide, and filling the petri-dish with dd H_2O. Incubate in dd H_2O at RT and protect from light for 3 × 15 minutes, or until expanded.

TROUBLESHOOTING

Imaging

18 Mount the tissue-hydrogel for imaging.

CRITICAL STEP The AcAm-embedded section must be mounted in, for example agarose, to prevent sample drift during imaging. Also, the mounted sample must be sealed between the coverslip and glass slide so that the water content of the agarose and of the expanded AcAM tissue-hydrogel remains at a steady-state. Otherwise, the sample will shrink from dehydration and/or expand when it absorbs water from the agarose (i.e. if placed in a humidity chamber).

19 Prepare 2% agarose in dd H_2O; cool solution until luke-warm and then add 0.01% sodium azide, if desired, for RT storage up to ~ 72 hours prior to imaging.

20 Pipette excess dd H_2O out of the petri-tissue containing the expanded sample and slide.

21 Center the sample on the large slide (within the petri-dish), and tissue away remaining dd H_2O with a Kimwipe.

22 Place a large coverslip on the sample without introducing air bubbles.

23 Pour 2% agarose onto one side of the slide, and allow the agarose to flow by capillary action between the slide and coverslip, encasing the sample. Continue pouring agarose until the sample is fully encased and there is no airspace between the slide and coverslip.

24 Once the agarose has set, use a razor blade or scalpel to slice along the coverslip edge and remove excess agarose.

25 Thickly paint Entellan or nail polish around the edge of the coverslip along the wall of agarose. This should seal the space between the slide and coverslip so that now air can seep into the agarose-mounted sample. This step is crucial. No water must be able to enter or leave

Nature Protocols: doi:10.1038/nprot.2015.122

the agarose + sample, or the sample's shape and size will fluctuate slowly during imaging. The water absorbed by the acrylate mounted sample must be at steady-state.

26 Once the seal is dry, vacuum grease may be used to reinforce the seal.

27 Image the cleared sample; if necessary, samples may be stored short-term at 4 °C.

ANTICIPATED RESULTS

Tissue size fluctuations can place undue stress upon cellular architecture[20], causing concern about utilizing tissue clearing procedures like ePACT. Indeed, we provide conclusive evidence that fine processes are compromised with unchecked expansion (see Fig. S4a-b, item 3). However, we have also found that tissue swelling may be used to great advantage in certain applications. As an example, certain cell populations are difficult to study due to their high density. To determine virus infectivity for AAV vector engineering or the expression level and coverage of an optogenetic construct, accurate and time-intensive cell-counting must often be performed in discrete tissue regions. For dense cell populations, such as the dopaminergic neurons of the ventral tegmental area and substantia nigra pars compacta, or the cells in the dentate gyrus, it may become difficult to distinguish and count fluorescently-labeled cells by hand, and the overlap of labeled cells makes automation of this process nontrivial. Finally, for circuit mapping according to the newly developed neuronal positioning system (NPS)[21], complications arise when there is spatial overlap of fluorescent NPS vesicles at the cell soma or poor spectral separation between NPS vesicles and endogenous Brainbow[22] labeling; the resolution and fluorescence intensity detection offered by confocal microscopy can be insufficient for positive cell identification and accurate projection tracing in these scenarios. The ePACT procedure, by clearing tissue through both SDS-based lipid removal and RI homogenization, can greatly assist in these circumstances. With respect to the latter, enzymatically digesting and inflating the tissue with water, such that proportionally less tissue volume is occupied by heterogeneous cellular components, serves to optically clear the tissue as well as to dilute the fluorescent, nonspecific and/or background signal. In turn, fluorescently labeled targets come into view (see Fig. S4a-b, items 1 and 2), and automated cell counting becomes possible.

Whereas figure S4 demonstrates that the ePACT technique is applicable to the "microscale" study of cellular morphology and cell populations, we believe that an additional future value lays in the nanoscale measurement of fluorescent probes in smFISH experiments. Our previous research[23] revealed that, even with the 1.5× expansion conveyed by standard PACT, single labeled transcripts were more readily discernable in PACT tissue than in the

Nature Protocols: doi:10.1038/nprot.2015.122

customary thin sections due to both lower background and their expansion-based separation. Instead, by utilizing the 4× tissue expansion conferred by ePACT to further enlarge the optical space within a cell (see Fig. S4c), quantitative analysis of multiple transcripts isolated to their subcellular locations can be more easily performed.

Troubleshooting ePACT

Step	Problem	Potential Cause	Suggested Solution
Expansion (step 17)	The section ripples or puckers as it expands	Collagenase digestion (step 16) was insufficient	Rinse the section in TESCA, and repeat step 16. Prepare fresh collagenase to ensure full enzyme activity, and replace collagenase digestion buffer with fresh, half-way through the digestion.
	The tissue cracks during expansion	Insufficient clearing, such that collagenase cannot access all tissue during digestion	Transfer the section back to 10% SDS-BB (pH 8.5) and clear for several hours as in steps 13-15. If tissue begins to expand evenly during washing – proceed to step 17. If not, repeat the collagenase digestion step 16, too.
		Insufficient tissue permeabilization (step 2A.v or 2B.iii), which impedes the diffusion of SDS micelles during clearing	Perform a more rigorous permeabilization step after fixing the tissue (PBST with 1% Triton X-100); always perform a freeze-thaw step as part of the permeabilization regimen.

Nature Protocols: doi:10.1038/nprot.2015.122

PACT clearing as applied to RNA FISH

Table 4

BACKGROUND

The following protocol briefly summarizes the application of PACT-cleared 100 μm thick tissues to RNA fluorescence in-situ hybridization studies (FISH), which was first presented in Yang *et al.*[23] It should be noted that there are several well-written and detailed articles on FISH and single-molecule (sm) FISH within *Nature Protocols*[24,25] and *Nature Methods*[26-30] that discuss the specifics of these techniques, including their usage in a variety of model systems, the design of RNA and DNA probes[31,32], methods for super-resolution barcoding of multiple transcripts within single-cells[33], and the quantification of labeled transcripts.

REAGENTS

- 100 μm PACT-cleared tissue sections

CRITICAL Samples may be embedded in A4P0 provided that the hydrogel is rigorously degassed, or in hydrogel formulations containing PFA, such as A4P1, and/or bis-acrylamide, such as A4P1B0.05. The increased degree of crosslinking in PFA- and bis-acrylamide-containing tissue-hydrogel hybrids will more effectively trap nucleic acid transcripts in the sample, promoting their retention during clearing and labeling steps.

- PBS, pH 7.4, RNase-free, 10× (Life Technologies, cat. no. AM9625)
- Ethanol, absolute (J.T. Baker, cat. no. 8025)

CAUTION Ethanol is flammable.

- Sodium borohydride (Sigma-Aldrich, cat. no. 213462, or Santa Cruz biotechnology, cat. no. CAS 16940-66-2)

CAUTION Sodium borohydride is highly flammable when in contact with moisture and is very toxic to the skin. Do not leave the flask uncapped. Prepare dilutions fresh, on ice, in fume or chemical hood. Close it tightly after weighing, seal with parafilm, and return to its containment canister (if applicable to institutional laboratory practices).

- Dextran sulfate (Sigma-Aldrich, cat. no. D8906)
- Formamide, deionized, nuclease-free (EMD Millipore, cat. no. 344206; or Life Technologies, cat. no. AM9342)

CAUTION Formamide is a toxic chemical and a teratogen; handle it inside a fume hood with appropriate protective gear (gloves, goggles, lab coat).

- Saline sodium citrate (SSC), RNase-free, 20× (Life Technologies, cat. no. AM9763)

Nature Protocols: doi:10.1038/nprot.2015.122

- Sodium chloride (Sigma-Aldrich, cat. no. S3014)
- RNase-free sterile H_2O (Life Technologies, cat. no. 10977-015)
- FISH probes: 20mer oligo probes, 1 nM each per hybridization reaction and labeled with Alexa 594
- (see main protocol for extended reagents list for PACT-related experiments)

EQUIPMENT

- Microscope: Nikon Ti Eclipse microscope with an Andor Ikon-M camera and an Plan-Apo 60× 1.4 N.A. λ oil objective (w.d 0.13 mm) with an additional 1.5× magnification.
- Excitation lasers: (589 nm (SDL-589-XXXT), 532 nm (SDL-532-200TG) and 405nm(SDL-405-LM-030), all manufactured by Shanghai Dream Laser
- Aminosilane-treated coverslips: Coverslips were sequentially transferred between and sonicated in three solutions: first 1M NaOH, then 100% EtOH, and finally acetone. The cleaned coverslips were immediately submerged into a 2% solution of (3-Aminopropyl) triethoxysilane (Sigma 440140) in acetone for two minutes. Amine-modified coverslips were rinsed and stored in ultrapure water at RT [189].
- (see main protocol for extended equipment list for PACT-related experiments)

REAGENT SET-UP

- Ethanol dilutions: Prepare graded dilutions of 100%, 95%, 70% ethanol in RNase-free sterile H_2O.
- Permeabilization Buffer: Prepare a solution of 0.5% sodium borohydride (wt/vol) in 70% ethanol.
- 2× SSC: For 2× SSC, combine 100 ml 20× SSC with 850 ml RNase-free sterile H_2O, pH to 7.0, then add H_2O to a total volume of 1 L.
- 30% Formamide in 2× SSC: For 500 ml, combine 150 ml formamide with 50 ml 20× SSC and 300 ml RNase-free sterile H_2O, pH to 7.0.
- Hybridization buffer: Prepare 10% dextran sulfate (wt/vol, Sigma D8906), 10% formamide (vol/vol) in 2× SSC.

PROCEDURE

Sample Permeabilization prior to Hybridization

Nature Protocols: doi:10.1038/nprot.2015.122

1 Adhere PACT-cleared tissue sections to aminosilane-treated coverslips by dehydrating for 1 hour under light vacuum.

2 Wash samples twice in 100% ethanol for 10 minutes at RT.

3 Wash samples in 95% ethanol for 10 minutes at RT.

4 Incubate samples in 70% ethanol for 2 hours at 4 °C.

5 After incubation, place tissue in a 0.5% sodium borohydride (wt/vol) in 70% ethanol solution for 10 minutes at RT.

6 Rehydrate the tissue with 3 washes of 1× PBS.

Sample Hybridization

7 Perform overnight hybridizations at 37 °C in a hybridization buffer containing 1 nM per each of 24 Alexa 594 labeled 20mer oligo probes towards β-actin.

8 Wash samples in 30% formamide 2× SSC at RT for 30 minutes, followed by 4 washes with 2× SSC.

Sample Imaging

9 Mount the sample between two coverslips with Slowfade Gold + DAPI.

10 Image the sample. For example, in Yang *et al.*[23], 30 μm Z-stacks were acquired with a 0.5 μm step size.

Image Analysis

CRITICAL To analyze the acquired datasets, we use custom image analysis scripts written in MATLAB. Many transcript detection algorithms have been described previously[26,34,35].

11 Determine the average background of the sample. For example, the images[23] were median filtered using a 50 × 50 pixel kernel and the average pixel intensity of the center 200 × 200 pixel sub-image was used as the average background value of the image.

12 To detect smFISH dots, apply a Laplacian of Gaussian filter, thresholding the image based on the average background value and comparing the resulting image with a dilated image to find local maxima.

13 Calculate the error bars using the standard deviation of the resulting measurements.

Nature Protocols: doi:10.1038/nprot.2015.122

Supplementary Table S1. LSFM parts list.

Part	Vendor	Description	Catalog #
Laser	Changchun New Industries Optoelectronics Technology	Solid state laser 473 nm, 100 mW	MBLIII473
Laser	Thorlabs	HeNe laser 633 nm, 21 mW	HNL210L
Mirror	Thorlabs	1" broadband dielectric mirror, 400-750 nm	BB1-E02
Lens 1	Thorlabs	1/2" concave achromatic f=-50 mm doublet	ACN127-050-A
Lens 2	Thorlabs	1" convex achromatic f=150 mm doublet	AC254-150-A
Beam expander	Thorlabs	3X beam expander 400-640 nm	BE03M-A
Shutter	Uniblitz	Shutter 6 mm diameter	LS6T2
Shutter controller	Uniblitz	Shutter drive unit	VCM-DI
Galvanometer scanner	Cambridge Technology	XY galvanometer scanner with 6 mm mirrors	6215HSM40B
F-theta lens	Edmund Optics	Telecentric F-theta lens, 633 nm, 99.1 mm WD	NT64-426
Lens 3	Thorlabs	2" convex achromatic doublet f=100 mm	AC508-100-A
Lens 4	Thorlabs	1" convex achromatic doublet f=40 mm	AC254-040-A
Sample translation stage	ASI Imaging	MS2000 XYZ-theta motion stage, depth axis with linear encoder	XY S31121010FT, Z LS-50
Objective translation stage	Newport	XYZ ULTRAlign precision stage	561D-XYZ
Motorized translation stage actuator	Newport	12 mm range DC servo motor	TRB12CC
Actuator controller	Newport	DC servo controller	CONEX-CC
Objective lens	Olympus	25× 1.0NA multi-immersion	XLSLPLN25XGMP
Tube lens	Thorlabs	2" Achromatic doublet, various focal lengths	e.g. AC508-400-A-ML

Nature Protocols: doi:10.1038/nprot.2015.122

sCMOS camera	Andor	Light-sheet mode camera	Zyla 4.2
Oscilloscope	Tektronix	Oscilloscope 4-channels, 100 MHz	TDS2014C
Function generator	Tektronix	Dual-channel arbitrary function generator	AFG3022B
3D printer	Makerbot	Dual extrusion	Replicator 2X

Nature Protocols: doi:10.1038/nprot.2015.122

Supplementary References

1 Helmstaedter, M. *et al.* Connectomic reconstruction of the inner plexiform layer in the mouse retina. *Nature* **500**, 168-174 (2013).

2 Takemura, S.-y. *et al.* A visual motion detection circuit suggested by Drosophila connectomics. *Nature* **500**, 175-181 (2013).

3 Mikula, S., Binding, J. & Denk, W. Staining and embedding the whole mouse brain for electron microscopy. *Nat. Methods* **9**, 1198-1201 (2012).

4 Lakadamyali, M., Bates, M., Babcock, H., Lichtman, J. & Zhuang, X. Mapping Neuronal Connectivity Using Stochastic Optical Reconstruction Microscopy (Storm): The Brainstorm Project. *Biophys. J.* **98**, 214a (2010).

5 Lakadamyali, M., Babcock, H., Bates, M., Zhuang, X. W. & Lichtman, J. 3D multicolor super-resolution imaging offers improved accuracy in neuron tracing. *PLoS One* **7**, e30826 (2012).

6 Berning, S., Willig, K. I., Steffens, H., Dibaj, P. & Hell, S. W. Nanoscopy in a living mouse brain. *Science* **335**, 551 (2012).

7 Glenn, D. R. *et al.* Correlative light and electron microscopy using cathodoluminescence from nanoparticles with distinguishable colours. *Sci. Rep.* **2**, 865 (2012).

8 Tapia, J. C. *et al.* High-contrast en bloc staining of neuronal tissue for field emission scanning electron microscopy. *Nat. Protoc.* **7**, 193-206 (2012).

9 Hayworth, K. J. *et al.* Ultrastructurally smooth thick partitioning and volume stitching for large-scale connectomics. *Nat. Methods* **12**, 319-U355 (2015).

10 Lichtman, J. W., Pfister, H. & Shavit, N. The big data challenges of connectomics. *Nat. Neurosci.* **17**, 1448-1454 (2014).

11 Helmstaedter, M. Cellular-resolution connectomics: challenges of dense neural circuit reconstruction. *Nat. Methods* **10**, 501-507 (2013).

12 Marx, V. Neurobiology: Brain mapping in high resolution. *Nature* **503**, 147-152 (2013).

13 Ladinsky, M. S. & Howell, K. E. Electron tomography of immunolabeled cryosections. *Methods Cell Biol.* **79**, 543-558 (2007).

14 Mastronarde, D. N. Automated electron microscope tomography using robust prediction of specimen movements. *J. Struct. Biol.* **152**, 36-51 (2005).

15 Mastronarde, D. N. Correction for non-perpendicularity of beam and tilt axis in tomographic reconstructions with the IMOD package. *J. Microsc.* **230**, 212-217 (2008).

16 Khandelwal, S. & Saxena, R. K. Age-dependent increase in green autofluorescence of blood erythrocytes. *J. Biosci.* **32**, 1139-1145 (2007).

Nature Protocols: doi:10.1038/nprot.2015.122

17 Schnell, S. A., Staines, W. A. & Wessendorf, M. W. Reduction of lipofuscin-like autofluorescence in fluorescently labeled tissue. *J. Histochem. Cytochem.* **47**, 719-730 (1999).

18 Klikugawa, K., Beppu, M. & Sato, A. Extraction and purification of yellow-fluorescent lipofuscin in rat kidney. *Gerontology* **41**, 1-12 (1995).

19 Kupferschmidt, D. A., Cody, P. A., Lovinger, D. M. & Davis, M. I. Brain BLAQ: Post-hoc thick-section histochemistry for localizing optogenetic constructs in neurons and their distal terminals. *Front. Neuroanat.* **9** (2015).

20 Grace, A. A. & Llinas, R. Morphological artifacts induced in intracellularly stained neurons by dehydration: Circumvention using rapid dimethyl sulfoxide clearing. *Neuroscience* **16**, 461–475 (1985).

21 Tsuriel, S., Gudes, S., Draft, R. W., Binshtok, A. M. & Lichtman, J. W. Multispectral labeling technique to map many neighboring axonal projections in the same tissue. *Nat. Methods* **12**, 547-552 (2015).

22 Livet, J. *et al.* Transgenic strategies for combinatorial expression of fluorescent proteins in the nervous system. *Nature* **450**, 56-62 (2007).

23 Yang, B. *et al.* Single-cell phenotyping within transparent intact tissue through whole-body clearing. *Cell* **158**, 945-958 (2014).

24 Skinner, S. O., Sepúlveda, L. A., Xu, H. & Golding, I. Measuring mRNA copy number in individual Escherichia coli cells using single-molecule fluorescent in situ hybridization. *Nat. Protoc.* **8**, 1100-1113 (2013).

25 Lyubimova, A. *et al.* Single-molecule mRNA detection and counting in mammalian tissue. *Nat. Protoc.* **8**, 1743-1758 (2013).

26 Lubeck, E. & Cai, L. Single-cell systems biology by super-resolution imaging and combinatorial labeling. *Nat. Methods* **9**, 743-748 (2012).

27 Lubeck, E., Coskun, A. F., Zhiyentayev, T., Ahmad, M. & Cai, L. Single-cell in situ RNA profiling by sequential hybridization. *Nat. Methods* **11**, 360-361 (2014).

28 Ke, R. *et al.* In situ sequencing for RNA analysis in preserved tissue and cells. *Nat. Methods* **10**, 857-860 (2013).

29 Levesque, M. J., Ginart, P., Wei, Y. & Raj, A. Visualizing SNVs to quantify allele-specific expression in single cells. *Nat. Methods* **10**, 865-867 (2013).

30 Levesque, M. J. & Raj, A. Single-chromosome transcriptional profiling reveals chromosomal gene expression regulation. *Nat. Methods* **10**, 246-248 (2013).

Nature Protocols: doi:10.1038/nprot.2015.122

31 Choi, H. M. T., Beck, V. A. & Pierce, N. A. Next-Generation in Situ Hybridization Chain Reaction: Higher Gain, Lower Cost, Greater Durability. *ACS Nano.* **8**, 4284-4294 (2014).

32 Choi, H. M. *et al.* Programmable in situ amplification for multiplexed imaging of mRNA expression. *Nat. Biotechnol.* **28**, 1208-1212 (2010).

33 Cai, L. Turning single cells into microarrays by super-resolution barcoding. *Brief. Funct. Genomics* **12**, 75-80 (2013).

34 Femino, A. M., Fay, F. S., Fogarty, K. & Singer, R. H. Visualization of Single RNA Transcripts in Situ. *Science* **280**, 585-590 (1998).

35 Itzkovitz, S. *et al.* Single-molecule transcript counting of stem-cell markers in the mouse intestine. *Nat. Cell Biol.* **14**, 106-114 (2012).

Nature Protocols: doi:10.1038/nprot.2015.122